NIH Public Access
Author Manuscript
Adv Mater. Author manuscript; available in PMC 2014 April 02.

Published in final edited form as:
Adv Mater. 2011 August 2; 23(29): 3278–3283. doi:10.1002/adma.201100821.

Dynamic Topographical Control of Mesenchymal Stem Cells by Culture on Responsive Poly(ε-caprolactone) Surfaces

Duy M. Le,
Department of Chemistry, University of North Carolina, Chapel Hill, NC 27599 (USA)

Dr. Karina Kulangara,
Department of Biomedical Engineering, Duke University, Durham, NC 27710 (USA)

Andrew F. Adler,
Department of Biomedical Engineering, Duke University, Durham, NC 27710 (USA)

Professor Kam W. Leong, and
Department of Biomedical Engineering, Duke University, Durham, NC 27710 (USA)

Professor Valerie Sheares Ashby
Department of Chemistry, University of North Carolina, Chapel Hill, NC 27599 (USA)

Kam W. Leong: kam.leong@duke.edu; Valerie Sheares Ashby: ashby@email.unc.edu

Keywords

Shape memory polymers; Dynamic cell culture; Surface topography; Mesenchymal stem cell; Polycaprolactone

There is clear, emerging evidence in the literature supporting the influence of surface topography on various cell phenotypes.[1–5] Recent advancements in mechanobiology have relied heavily on synthetic extracellular matrix (ECM) mimics to investigate how cellular phenomena are dependent upon surface geometry. Concurrent developments in micro/nano-fabrication techniques have enabled the construction of well-defined surface arrays which aim to emulate the extracellular microenvironment.[6] Numerous patterns of different sizes and shapes including grooves, posts, and pits have been used to study the *in vitro* response of various cell types such as: fibroblasts, osteoblasts, epithelial cells, neuronal cells, and more recently stem cells.[7–14]

Cell-topography interactions have far-reaching implications in cell biology and biomedical engineering. Many biological processes such as embryogenesis and angiogenesis are strongly influenced by these interactions.[4,15,16] Additionally, abnormalities in ECM sensing have been linked to many disease states such as cardiomyopathy, muscular dystrophy, and oncogenesis.[17–19] Topography is also currently being explored as a means to mechanically direct stem cell fate and will be important in the design of next generation tissue engineering scaffolds.[13,20–23] However, there remain significant fundamental questions surrounding cell-topography interactions for which innovative, dynamic biomaterials may offer new insights not previously accessible by static substrates. Accordingly, there has been an increased effort to design dynamic substrates that can communicate active physical cues to cells in a more biomimetic context.[24–28]

Correspondence to: Valerie Sheares Ashby, `ashby@email.unc.edu`.

Supporting Information is available online from Wiley InterScience or from the author.

Takayama first demonstrated the application of dynamic topography to cultured cells using reversible poly(dimethylsiloxane) (PDMS) surfaces.[29] Reversible wavy micro-features were fabricated by subjecting the PDMS surfaces to plasma oxidation and subsequently applying compressive stress to induce surface buckling. The study provided evidence that C2C12 myoblast cell morphology can be directed dynamically using surface array transitions. While these preliminary findings are innovative, the suitability of these materials for dynamic *in vitro* analysis is constrained by poor replication fidelity, batch variability, low feature resolution, and limited shape versatility. An alternative approach to fabricating reversible surface features is by exploiting the unique properties of shape memory polymers (SMPs). These materials can change shape in a predetermined way when exposed to the appropriate stimulus. Shape retention and recovery are typically facilitated through the highest thermally-reversible phase transition of the polymer. This transition temperature (T_{trans}) is closely associated with the polymer glass transition temperature (T_g) or melting temperature (T_m).[30] Recently, Henderson reported the control of fibroblast cell alignment and microfilament organization using reversible grooved micro-structures embossed into NOA-63, a polyurethane-based thiol-ene crosslinked SMP.[31] The study demonstrated that SMPs enable a high degree of control over the activation of the surface shape memory effect. However, the large, irregular dimensions of the surface patterns limited the degree of control over fibroblast cell morphology. Developing strategies that enable strict regulation of the shape memory effect and precise control over surface geometry with sub-cellular resolution remains a great challenge for dynamic cell culture applications.

We are interested in addressing these limitations by engineering biocompatible shape memory surfaces that can accomodate diverse, well-defined, and biologically relevent surface transformations under physiological conditions. To this end, thermally responsive poly(ε-caprolactone) (PCL) SMP surfaces were developed for the purpose of dynamically probing cell-topography interactions. PCL was chosen based on its known biocompatibility and exceptional shape memory properties.[32,33] Star-shaped PCL triols were synthesized by glycerol initiated bulk ring-opening polymerization of ε-caprolactone in the presence of tin octanoate. Control over molecular weight ($\langle M_n \rangle$) could be achieved by manipulating the monomer to initiator stoichiometry. The resulting telechelic prepolymers showed excellent agreement with the target $\langle M_n \rangle$ values and yielded narrow polydispersity indices (PDI ≤ 1.2) (Supporting Information (SI), Table S1). The oligo-precursors were methacrylate end-functionalized and subsequently crosslinked by photo-initiated free radical polymerization in the melt. The synthetic route to PCL SMP networks from 3-arm oligo-precursors is shown in the supporting information, Figure S1. Differential scanning calorimetry (DSC) showed a systematic dependence of the network T_m on the $\langle M_n \rangle$ of the prepolymers. Increasing the chain length promoted the formation of larger and more stable PCL crystallites and consequently a higher T_m. This was reflected through the heat of fusion (ΔH_m) and degree of crystallinity (χ_c) which also demonstrated a concomitant increase with increasing chain length. PCL networks synthesized from 12,500 gmol^{-1} star-shaped prepolymers (PCLx-12500) showed a ΔH_m, χ_c, and T_m of 30.5 Jg^{-1}, 22 %, and 36 °C, respectively (SI, Table S2). Activation of the shape memory effect near physiological temperature (37 °C) is critical for effective dynamic cell culture. Clinical trials for hyperthermic treatments are typically applied at 42 °C for 30 minutes.[34] For this reason, shape memory activation at temperatures between 35 and 41 °C were designated as ideal to mitigate heat shock and significant cell death. A T_{trans} near physiological temperature was achieved through judicious control over $\langle M_n \rangle$ and the selection of a branched prepolymer architecture, as several studies have shown that highly branched polyesters can possess T_m values much lower than those attainable by their linear counterparts.[35–38]

A shape memory cycle begins by crosslinking liquid prepolymer into the desired primary shape. The primary shape is then mechanically deformed into a secondary shape at temperatures which exceed T_{trans}. Subsequently, the sample is cooled below T_{trans} while still under mechanical load to induce crystallization. Consequently, the secondary shape is retained through a sharp reduction in molecular mobility. Recovery of the original shape is then attained by simply heating the unconstrained network above T_{trans}.[39] The resulting increase in polymer chain mobility allows the entropic energy lost during deformation to be converted into a restorative force that reestablishes the original shape of the network.[40] The fabrication process is shown in Figure 1.[41,42] Soft replica molds of a silicon master were used in concert with specific thermomechanical cycles to program the primary and secondary surface arrays. Figure 2 shows three surface array transformations between various secondary and recovered (40 °C in water) topographies. Primary shapes (a, d, and g) are also shown for visual comparison to recovered topographies (c, f, and i). The surfaces transformations are as follows: (b–c) 2 μm cubes to 3 × 1 μm hexnuts, (e–f) 7 × 14 μm cylinders to 10 × 1 μm boomerangs, and (h–i) 3 × 5 μm channels to a planar topography. The PCL surfaces demonstrated excellent replication fidelity, secondary shape retention, and primary shape recovery. Using this method a library of surface transformations can be achieved with exquisite control over surface feature size and geometry. The fabrication technique can also be readily adapted to include submicron-topographies which have been shown to exert a more pronounced effect on cell behavior than micro-topography.[13]

Shape memory performance was analyzed quantitatively by thermomechanical tensile analysis. The most common figures of merit for shape memory performance are the shape fixity (R_f) and shape recovery (R_r) ratios. R_f is a measure of secondary shape retention, while R_r is an evaluation of primary shape recovery. PCL films (1 × 37 × 3 mm) were heated to 60 °C and extended to a total fixed strain (ε_m) of 35 %. The sample was then allowed to cool under load to room temperature. Subsequently, the stress was removed and the strain observed after unloading (ε_u) was recorded to determine R_f. The primary shape was recovered by immersing the substrates in a 40 °C water bath for 10 min. The permanent strain after recovery (ε_p) was measured to calculate R_r. Under these conditions PCLx-12500 showed excellent shape memory properties with near quantitative R_f and R_r values of 99% and 98%, respectively (SI, Table S3).

In addition to excellent thermal and mechanical properties, SMP biomaterials must also possess optimized surface properties for cell adhesion. To improve cell attachment the PCL films were oxygen plasma-treated to reduce the static contact angle from approximately 90° to 40° (Figure 3a). Oxygen plasma treatment is an ideal method of post-polymerization surface modification as it effectively decreases hydrophobicity through the introduction of oxygen containing groups to the surface without disturbing the bulk thermal and mechanical properties.[43] The improved wettability of oxygen plasma-treated polymers has been shown to enhance the adsorption of cell adhesion proteins such as fibronectin (Fn). Additionally, hydrophilic surfaces are known to favor the active conformational states of adhesion proteins which also leads to enhanced cell attachment.[44] Thus, to further encourage cell adhesion, the oxygen plasma-treated films were coated with Fn. Green fluorescence protein transduced-human mesenchymal stem cells (GFP-hMSCs) were cultured on untreated, oxygen plasma, and oxygen plasma-Fn modified planar PCL surfaces in addition to tissue culture poly(styrene) (TCPS) as the control (Figure 3b–e). It was clearly shown that the oxygen plasma treatment (Figure 3d) substantially increased cell attachment over untreated (Figure 3c) PCL surfaces. Additional Fn modification of oxygen plasma-treated surfaces (Figure 3e) resulted in a more pronounced effect on cell attachment, with cell densities comparable to that of the TCPS control (Figure 3b).

Cytotoxicity was evaluated by WST-1 cell proliferation assay. Surface modified PCL substrates demonstrated a much higher cell viability than untreated PCL materials. hMSCs cultured on untreated and oxygen plasma-Fn modified planar PCL surfaces demonstrated a

38% and 80% cell viability, respectively. In conjunction to cell viability, immunofluorescent staining of the actin cytoskeleton (488 phalloidin-Oregon Green, DAPI nuclear counter-staining) showed the hMSCs were able to establish normal, healthly cell morphology on static PCL planar surfaces and on 2 μm cubic arrays (Figure 3 f–g) Although the cell shown in Figure 3g is healthy, its appearance is atypical. This is the result of cell morphology changes in response to substrate topography, as has been previously shown in the literature.[13, 23]

Finally, to demonstrate the potential of PCL SMP surfaces in dictating cell morphology, GFP-hMSCs were cultured on dynamic PCL surfaces at 28 °C for 1 day, after which, the cells were subjected to the surface shape memory effect at 40 °C for 1h and subsequently allowed to equilibrate at 37 °C for 12 h. Fluorescent microscopy revealed that cells cultured on static planar PCL control surfaces demonstrated a stellate shaped morphology before heat treatment (Figure 4a). When subjected to the heat treatment the morphology of the cells remained stellate shaped (Figure 4b). GFP-hMSCs cultured on static 3 × 5 μm channel control arrays demonstrated marked cell alignment along the major axis of the anisotropic surface features, a phenomena commonly known as contact guidance (Figure 4c).[45] No change in cell morphology was observed when the aligned cells were heated on the static channels (Figure 4d). GFP-hMSCs cultured on temporary 3 × 5 μm channel arrays also demonstrated significant cell alignment (Figure 4e). The surface shape memory effect was activated by culturing the adherent cells at 40 °C in hMSC growth media (hMSCGM) for 1 hour resulting in the rapid dissipation of the secondary channel topography and the recovery of the primary planar topography. After the cells were allowed to equilibrate for 12 h the hMSCs returned to a stellate shaped morphology (Figure 4f).

Widefield image analysis was performed to quantify cell orientation and alignment (Figure 5). Three images were collected from each of three replicates for static planar, static channels, and SMP surfaces (3 × 5 μm channels to planar topography) at 28 °C and 37 °C. The angle of deviation from the horizontal axis was measured for each, with 0° (90°) denoting a cell parallel (perpendicular) to the channel direction. An average angle of deviation of 45° represents a random orientation with respect to the horizontal axis. GFP-hMSCs cultured on static planar PCL surfaces at 28 °C demonstrated a completely random (45°) cell orientation. There was no statistical difference between cell orientations on static planar surfaces before and after the heat treatment. In contrast, cells cultured on static channel arrays at 28 °C demonstrated marked cell alignment corresponding to a 10° average angle deviation from the channel axis. Following the heat treatment and equilibration period, the average angle deviation from the channel axis rose slightly, indicating a reduction in cell alignment. These findings can be accounted for by heat induced cell death of hMSCs cultured on channel topographies which resulted in cell rounding and a minor loss in cell alignment. hMSCs cultured on a temporary channel topography at 28 °C showed no statistical difference with cells cultured on static channel surfaces at the same temperature. A completely random average cell orientation was not observed for recovered planar surfaces due to defects inflicted on the SMP surface during thermomechanical processing. However, the surface transformation to a planar topography did result in a significant increase in average angle deviation in comparison to the temporary channel topography.

These results indicate that the morphology of GFP-hMSCs can be topographically dictated through the application of the surface shape memory effect between 3 × 5 μm channels to a flat topography under physiological conditions. Moreover, SMP cell culture platforms described here provide a highly versatile and controlled means of probing cellular response to localized changes in topography. These materials possess feature resolution, sharpness, and variability that have not previously been reported in the literature for SMP surfaces. These findings may have far-reaching implications in investigating the effect of dynamic topography on cell adhesion, cytoskeletal organization, cell signaling, and mechanotransductive events.[46,47]

In summary, the present study describes the synthesis, characterization, and application of thermally-responsive PCL SMP micro-arrays to dynamic cell culture. The PCL thermosets demonstrated excellent mechanical properties, a body temperature T_{trans}, and near quantitative R_f and R_r. Oxygen plasma-Fn modified SMP surfaces supported hMSC culture with good attachment efficiency, normal cell morphology, and minimal cytotoxicity. The hMSC morphology switched from highly aligned to stellate shaped in response to a surface transformation between a 3 × 5 μm channel array and a planar surface at 37 °C. This on-demand, surface directed change in cell morphology offers a novel means to study cell-topography interactions with unprecedented control over surface feature size and geometry and may represent a generally applicable method to investigate a wide variety of topography mediated changes in cell behavior.

Experimental

Polymer synthesis and network fabrication

ε-Caprolactone (99%), tin octanoate, and anhydrous glycerol were purchased from Sigma-Aldrich. Acetic acid, methylene chloride, methanol, and acetone were purchased from Fisher Scientific. ε-Caprolactone was dried over CaH_2 for 24 h and distilled prior to use. Perfluoropolyether (PFPE) and PDMS molds were prepared in house. Star-shaped PCL prepolymers were synthesized by bulk ring opening polymerization of ε-caprolactone using tin octanoate and the trifunctional glycerol initiator. Under nitrogen atmosphere, glycerol, tin octanoate, and ε-caprolactone were added to the reaction vessel and heated to 120 °C for 2.5 h, whereupon the reaction was quenched with acetic acid, and the product was precipitated in cold (−78 °C) methanol. Subsequently, the oligo-PCL was refluxed with 4.5 mol equivalents of 2-isocyanatoethyl methacrylate and 0.1 mol % tin octanoate in anhydrous methylene chloride. PCL networks were prepared by casting molten PCL trimethacrylate precursor and photoinitiator diethoxyacetophenone (DEAP) (0.1 wt %) into a teflon mold. Subsequently, the molten PCL was irradiated with 30 mW/cm^2 UV light (365 nm) under N_2 atmosphere for 10 min. PFPE and PDMS replica molds were used as photo-curing templates or to emboss secondary surface patterns. Mechanical force was applied at 130 °C for 15 min followed by rapid cooling to −78 °C for an additional 60 min. The primary, secondary, and thermally recovered shapes (40 °C) were imaged using brightfield microscopy.

Thermal and Thermomechanical Characterization

Thermal characterization was performed on a TA instrument Q200 differential scanning calorimeter (DSC), under nitrogen atmosphere from −20 °C to 80 °C with heating and cooling rates of 5 °C/min and 10 °C/min, respectively.

Shape memory performance was analyzed by thermomechanical tensile analysis using an Instron analyzer. The equations for R_f and R_r are as follows:

$$R_f=\frac{\varepsilon_u}{\varepsilon_m}\cdot 100 \quad (1)$$

$$R_r=\frac{\varepsilon_u-\varepsilon_p}{\varepsilon_m-\varepsilon_p}\cdot 100 \quad (2)$$

R_f is defined as the fixed strain after unloading (ε_u) to the total strain induced during deformation (ε_m). R_r is defined as the ratio of the difference between the strain after unloading (ε_u) and the permanent strain after recovery (ε_p) to the difference between the total strain induced during deformation (ε_m) and the permanent strain after recovery (ε_p).[48] Dog bone molds (1 × 37 × 3 mm) were heated to 60 °C and extended to a strain of 35%. The sample was then allowed to cool under load to room temperature. Subsequently, the load was removed and the fixed strain was recorded to determine the shape fixity (R_f). To measure shape recovery (R_r), the polymer sample was immersed in water at 40 °C for 10 min.

Surface Modification and Characterization

The PCL substrates were modified by oxygen plasma treatment in an AutoGlow oxygen plasma system by Glow Research. Oxygen pressure was maintained at 1.3 mbar while the PCL substrates were subjected to 30 W of power intensity for 1 min. Prior to cell seeding, films were sterilized with UV light for 10 min per side. The PCL films were conditioned first by incubating in PBS buffer (1X) for 2 h. Subsequently, the substrates were immersed in 1 mL of 0.005 mg/mL fibronectin solution for 1 h. Surface hydrophobicity was evaluated by static water contact angle measurements. Contact angle was acquired using a KSV Instruments Cam 200 Optical goniometer using the sessile drop method.

Cytoxicity and Immunofluorescent Staining

hMSCs were cultured on featureless PCL substrates for 24 h. The materials were then transferred to new 24 well plates and immersed in fresh MSCGM and WST-1 reagent. The cells were then incubated at 37 °C for 1h. Cell proliferation was detected using UV-vis spectroscopy. Wells with no substrate and ethanol-treated cells were used as controls. For immunofluorescent staining, samples were fixed using 4% *p*-formaldehyde, permeablized with 0.1% TritonX-100 in phosphate buffered saline (PBS), and then blocked with 10% goat serum in PBS. F-actin was fluorescently labeled in fixed samples with Oregon Green 488 phalloidin (Molecular Probes, Eugene, OR), and the nucleus was counter-stained with 4′,6-diamidino-2-phenylindole (DAPI, Molecular Probes). Samples were imaged by confocal microscopy (Zeiss 510 inverted confocal microscope).

Human Mesenchymal Stem Cell Culture

Human MSCs were supplied by Dr. D. Prockop from Tulane Center for Gene Therapy at Tulane University, New Orleans, LA, USA. The hMSCs used in the experiments were at passages 3–6. hMSCs were cultured in complete culture media (CCM) comprising α-Minimum Essential Medium (α-MEM) supplemented with 16.5% (v/v) fetal bovine serum (FBS, Atlanta Biologicals, Inc., Lawrenceville, GA, USA), 2 mM L-glutamine (Gibco/Invitrogen, Carlsbad, CA, USA), 100 U/ml penicillin, and 100 mg/ml streptomycin (Gibco/Invitrogen, Carlsbad, CA, USA). The cells were seeded at a density of 10,500 cells/cm^2 and placed in an incubator under 5% CO_2.

Dynamic cell culture

GFP-hMSCs were seeded on static planar and static channel arrays as the controls. GFP-hMSCs were also cultured on shape memory surfaces with a temporary shape of 3 × 5 channels and a planar primary shape. The cells were cultured at 28 °C for 1 day, subsequently, the cells were subjected to a 40 °C heat treatment in hMSCGM for 1h. The cells were then allowed to equlibrate at 37 °C for 12 h.

Widefield image analysis of cell alignment

Images for quantification of GFP-hMSC alignment were acquired using a Nikon Eclipse TE2000-U fluorescence inverted microscope. Three images were collected from each of three replicate substrates – static planar, static channels, and SMP channels – at 28 °C, and 37 °C. Approximately 2,000 cells were analyzed for each condition using FIJI Macro, implemented by a tester blinded to the identity of each condition. Briefly, Bernsen's thresholding method was employed to define regions of high local contrast within each image, corresponding to the outline of each cell. Using FIJI's "Analyze Particles" command, ellipses were fit to these outlines, and an angle of deviation from the horizontal axis was measured for each, with 0° (90°) denoting a cell parallel (perpendicular) to the channel direction. Small (non-cell) particles were excluded with a size threshold. An average angle of deviation of 45° represents a random orientation with respect to the horizontal axis.

Statistical analysis

A global two-way ANOVA of cell alignment revealed significant main effects of temperature and substrate type, as well as of their interaction or the dependence of cell alignment on temperature as a function of substrate type ($p < 0.0001$ in each case). One-way ANOVAs with Bonferroni-corrected post-hoc testing was used to compare alignment between individual substrates at the same temperature conditions. Additionally, Student's t-tests were used to compare alignment between temperatures within each substrate condition.

Supplementary Material

Refer to Web version on PubMed Central for supplementary material.

Acknowledgments

Funding for this work was provided from NSF DMR grant 0418499, SNSF grant PA00P3_124163, and NIH grant 83008. The authors would like to thank the DeSimone lab at UNC-CH for digital renderings and PFPE materials. The authors would also like to thank Dr. Benjamin Pierce for discussion and insights.

References

1. Curtis A, Wilkinson C. Biomaterials. 1997; 18:1573. [PubMed: 9613804]
2. Martinez E, Lagunas A, Mills CA, Rodriguez-Segui S, Estevez M, Oberhansl S, Comelles J, Samitier J. Nanomedicine. 2009; 4:65. [PubMed: 19093897]
3. Flemming RG, Murphy CJ, Abrams GA, Goodman SL, Nealy PF. Biomaterials. 1999; 20:573. [PubMed: 10213360]
4. Yim EKF, Leong KW. Nanomedicine. 2005; 1:10. [PubMed: 17292053]
5. Bettinger CJ, Langer R, Borenstein JT. Angew Chem Int Edit. 2009; 48:2.
6. Hasirci V, Kenar H. Nanomedicine. 2006; 1:73. [PubMed: 17716211]
7. Yim EKF, Reano RM, Pang SW, Yee AF, Chem CS, Leong KW. Biomaterials. 2005; 26:5405. [PubMed: 15814139]
8. Curtis ASG, Casey B, Gallagher JO, Pasqui D, Wood MA, Wilkinson CDW. Biophys Chem. 2001; 94:275. [PubMed: 11804737]
9. Curtis ASG, Gadegaard N, Dalby MJ, Riehle MO, Wilkinson CDW, Aitchinson GA. IEEE Trans Nanobioscience. 2004; 3:61. [PubMed: 15382646]
10. Elias KL, Price RL, Webster TJ. Biomaterials. 2002; 23:3279. [PubMed: 12102199]
11. Bettinger CJ, Zhang Z, Gerecht S, Borenstein JT, Langer R. Adv Biomater. 2008; 20:99.
12. Johansson F, Carlberg P, Danielsen N, Montelius L, Kanje M. Biomaterials. 2006; 27:1251. [PubMed: 16143385]
13. Yim EKF, Pang SW, Leong KW. Exp Cell Res. 2007; 313:1820. [PubMed: 17428465]

14. Adler AF, Speidel AT, Christoforou N, Kolind K, Foss M, Leong KW. Biomaterials. 2011; 32:3611. [PubMed: 21334062]
15. Wozniak MA, Chen CS. Nat Rev Mol Cell Biol. 2009; 10:34. [PubMed: 19197330]
16. Ingber DE. FASEB J. 2006; 20:811. [PubMed: 16675838]
17. Jaalouk DE, Lammerding J. Nat Rev Mol Cell Biol. 2009; 10:63. [PubMed: 19197333]
18. Ingber DE. Differentiation. 2002; 70:547. [PubMed: 12492496]
19. Laconi E. Bioessays. 2007; 29:738. [PubMed: 17621638]
20. McNamara LE, McMurray RJ, Biggs MJP, Kantawong F, Oreffo ROC, Dalby MJ. Journal of Tissue Engineering. 2010; 2010:1.
21. Murray P, Edgar D. Phil Trans R Soc Lond B. 2004; 359:1009. [PubMed: 15306413]
22. Yim EKF, Darling EM, Kulangara K, Guilak F, Leong KW. Biomaterials. 2010; 31:1299. [PubMed: 19879643]
23. McBeath R, Pirone DM, Nelson CM, Bhadriraju K, Chen CS. Journal Dev Cell. 2004; 6:483.
24. Dartsch PC, Hämmerle H. Eur J Cell Biol. 1986; 41:339. [PubMed: 3530766]
25. Kloxin AM, Benton JA, Anseth KS. Biomaterials. 2010; 31:1. [PubMed: 19788947]
26. Lim HL, Chuang JC, Tran T, Aung A, Arya G, Varghese S. Adv Funt Mater. 2011; 21:55.
27. Grayson WL, Martens TP, Eng GM, Radisic M, Vunjak-Novakovic G. Semin Cell Dev Biol. 2009; 20:655.
28. Neuss S, Blomenkamp I, Stainforth R, Boltersdorf D, Jansen Marc, Butz N, Perez-Bouza A, Knüchel R. Biomaterials. 2009; 30:1697. [PubMed: 19121539]
29. Lam MT, Clem WC, Takayama S. Biomaterials. 2008; 29:1705. [PubMed: 18192004]
30. Lendlein A, Kelch S. Angew Chem Int Edit. 2002; 41:2034.
31. Davis KA, Burke KA, Mather PT, Henderson JH. Biomaterials. 2011; 32:2285. [PubMed: 21224032]
32. Lendlein A, Schmidt AM, Schroeter M, Langer R. J Poly Sci A. 2005; 43:1369.
33. Ping P, Wang W, Chen X, Jing X. Biomacromolecules. 2005; 6:1240.
34. Fajardo LF, Schreiber AB, Kelly NI, Hahn GM. Radiat Res. 1985; 103:276. [PubMed: 4023180]
35. Nagahama K, Ueda Y, Ouchi T, Ohya Y. Biomacromolecules. 2009; 10:1789. [PubMed: 19425546]
36. Xue L, Dai S, Li Z. Macromolecules. 2009; 42:964.
37. Finne A, Albertsson AC. Biomacromolecules. 2002; 3:684. [PubMed: 12099811]
38. Numata K, Srivastava RK, Finne-Wistrand A, Albertsson AC, Doi Y, Abe H. Biomacromolecules. 2007; 8:3115. [PubMed: 17722879]
39. Ratna D, Karger-Kocsis J. J Mater Sci. 2008; 43:254.
40. Cao F, Jana S. Polymer. 2007; 48:3790.
41. Williams SS, Retterer S, Lopez R, Ruiz R, Samulski ET, DeSimone JM. Nano Lett. 2010; 10:1421. [PubMed: 20178369]
42. Rolland JP, Hagberg EC, Denison GM, Carter KR, DeSimone JM. Angew Chem Int Edit. 2004; 43:5796.
43. Martins A, Pinho ED, Faria S, Pashkuleva I, Marques AP, Reis RL, Neves NM. Small. 2009; 5:1195. [PubMed: 19242938]
44. Yoshinari M, Wei J, Matsuzaka K, Inoue T. WASET. 2009; 58:171.
45. Kulangara K, Leong KW. Soft Matter. 2009; 5:4072.
46. Geiger B, Spatz JP, Bershadsky AD. Nature Rev Mol Cell Biol. 2009; 10:21. [PubMed: 19197329]
47. Wang N, Tytell JD, Ingber DE. Nature Rev Mol Cell Biol. 2009; 10:75. [PubMed: 19197334]
48. Mather PT, Xiaofan L, Rousseau IA. Annu Rev Mater Res. 2009; 39:445.
49. Peng P, Wang W, Chen X, Jing X. Biomacromolecules. 2005; 6:587. [PubMed: 15762617]

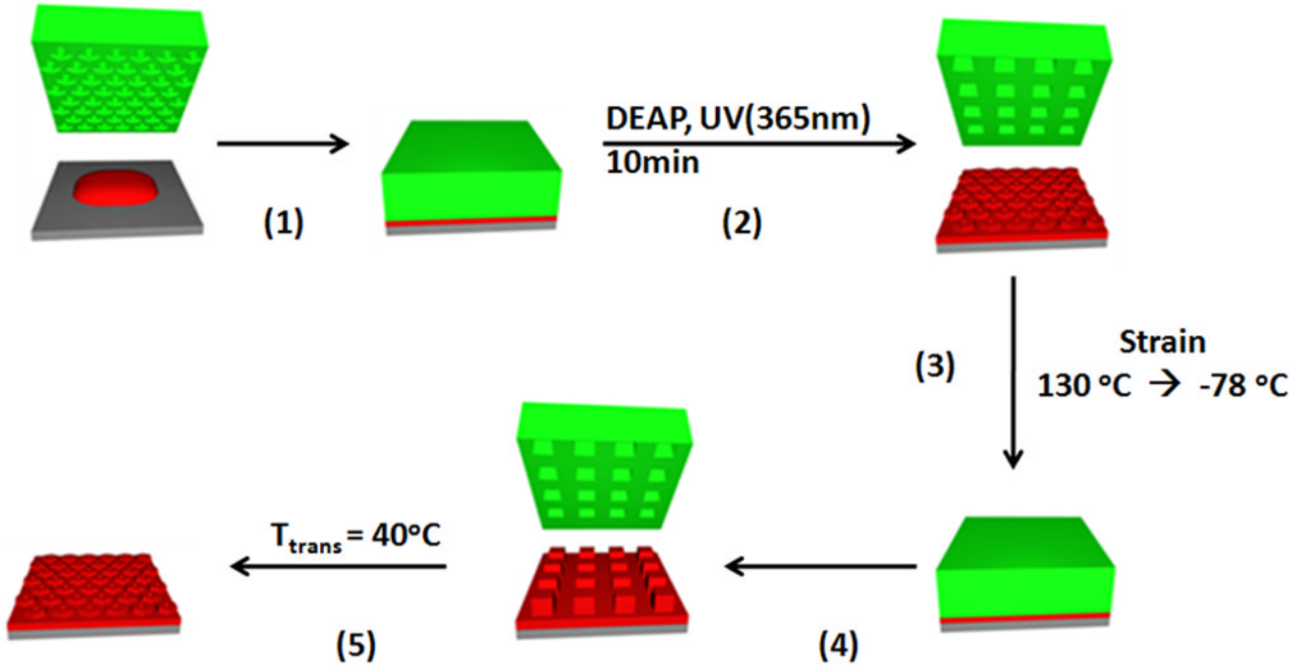

Figure 1.

Schematic representation of thermomechanical programming and recovery of shape memory surfaces. (1) The prepolymer in the melt was cast into a mold of the primary shape and (2) photo-cured using diethoxyacetophenone (DEAP) as the photo-radical initiator. (3) The primary shape was then mechanically deformed at 130 °C using a second replica mold and subsequently cooled to −78 °C while still under load. (4) To recover the primary shape, the compressive stress was removed and the polymer film was (5) immersed in water at 40 °C for 10 min.

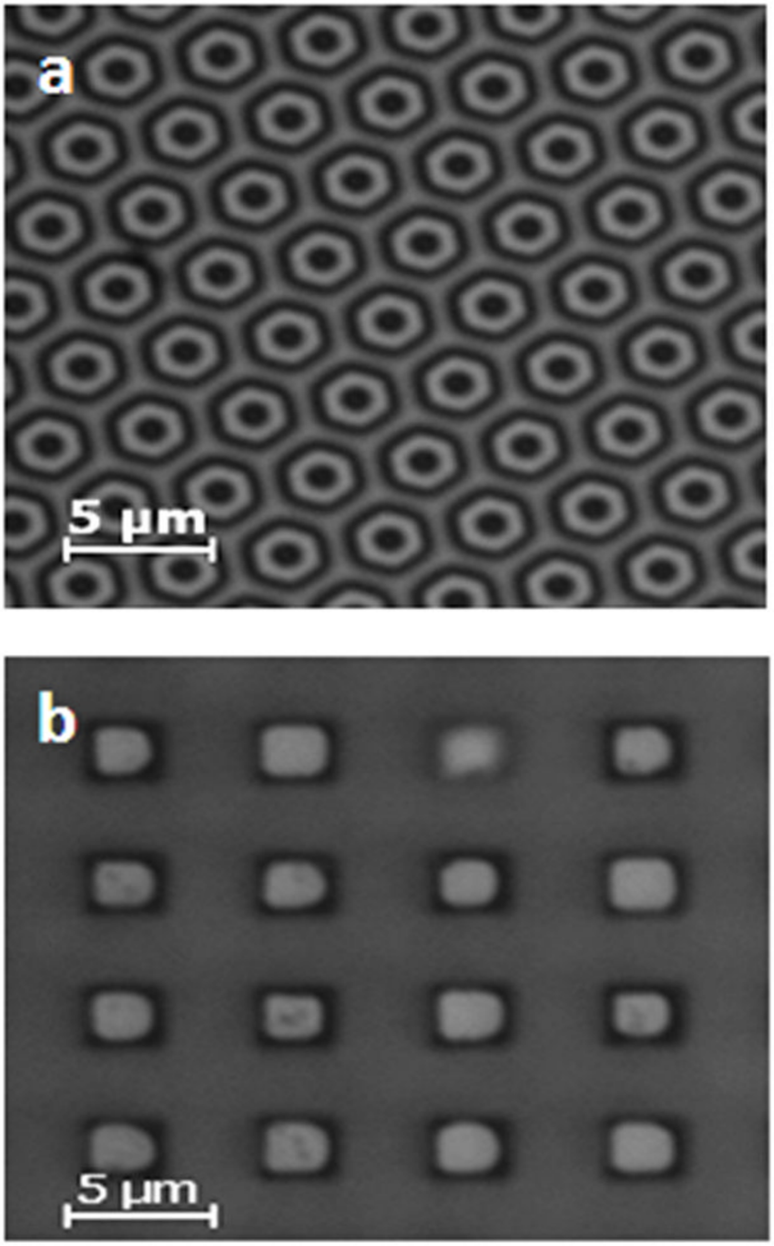
a
5 µm
b
5 µm

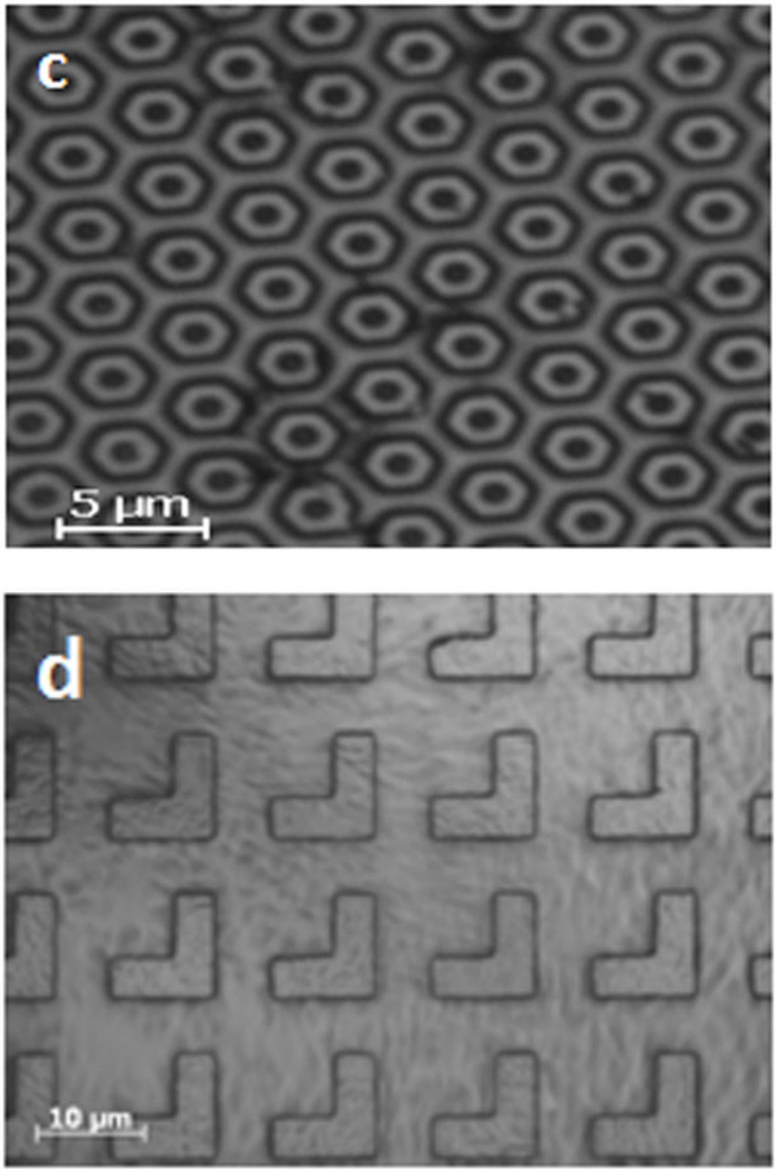
c
5 μm
d
10 μm

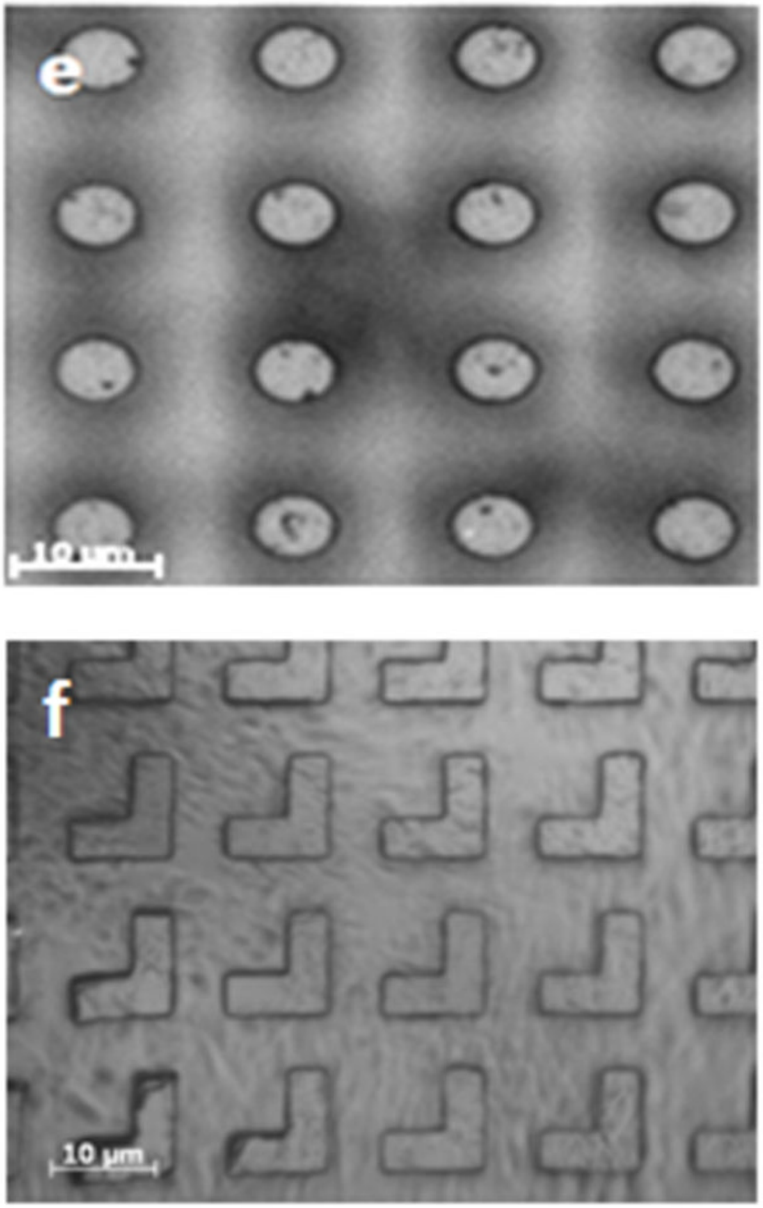
e
10 μm
f
10 μm

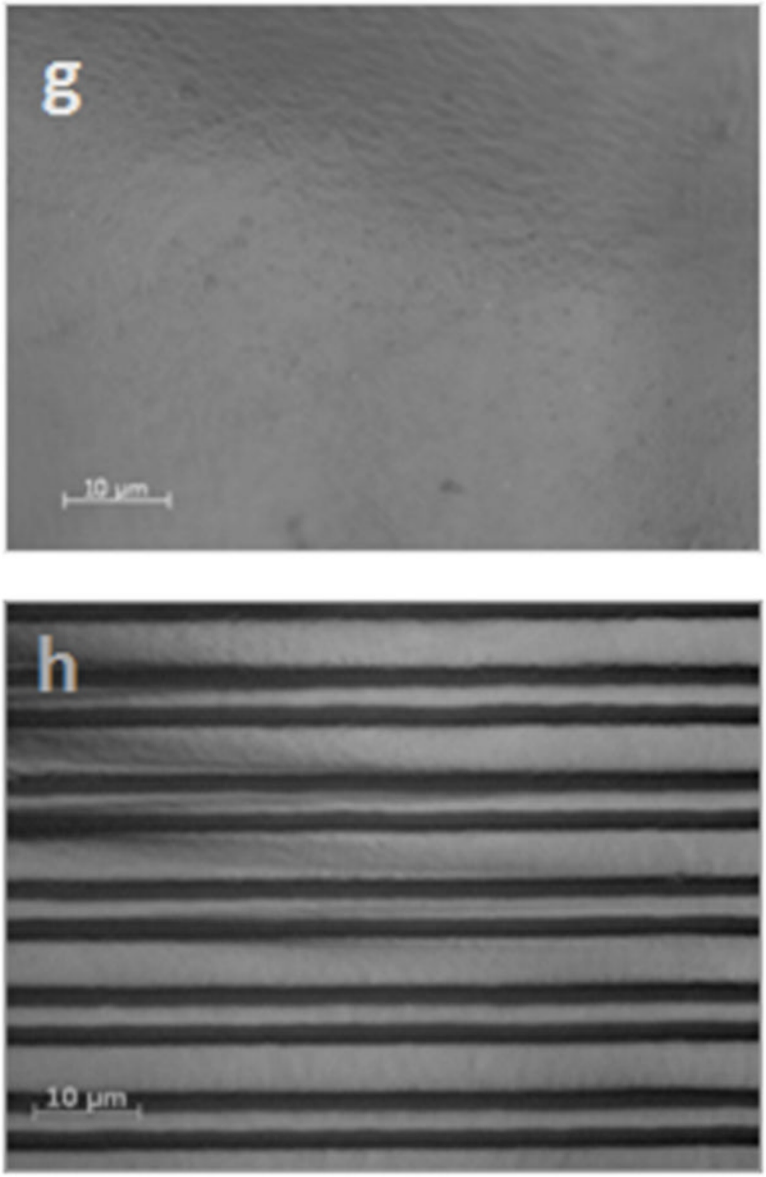
g
10 μm
h
10 μm

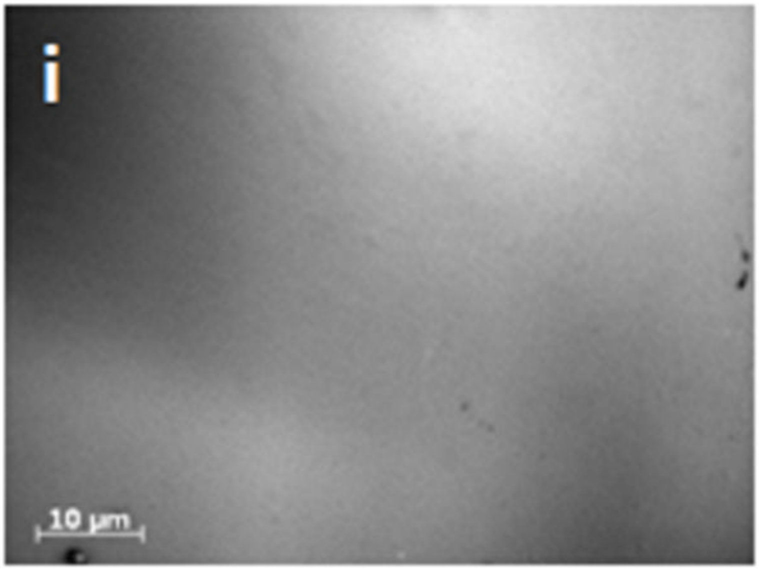

Figure 2.

Panning from left to right the primary, secondary and recovered shapes are shown. Brightfield images show surface transformations between various secondary and recovered (40 °C in water) topographies. Primary shapes (a, d, and g) are shown for visual comparison to recovered topographies (c,f, and i). The surface transformations are as follows: (b–c) 2 μm cubes to 3 × 1 μm hexnuts, (e–f) 7 × 14 μm cylinders to 10 × 1 μm boomerangs, and (h–i) 3 × 5 μm channels to planar topography. Scale bar is 5 μm (a–c) and 10 μm (d–i).

NIH-PA Author Manuscript NIH-PA Author Manuscript NIH-PA Author Manuscript

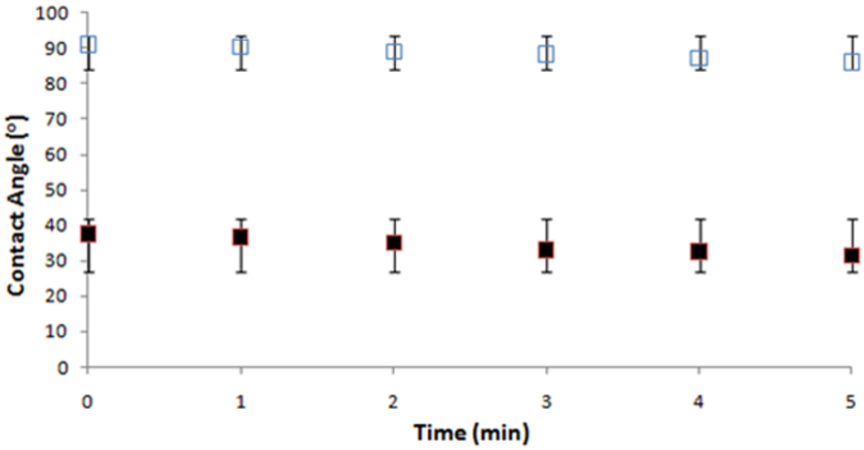
100
90
80
70
60
50
40
30
20
10
0
Contact Angle (°)
0
1
2
3
4
5
Time (min)

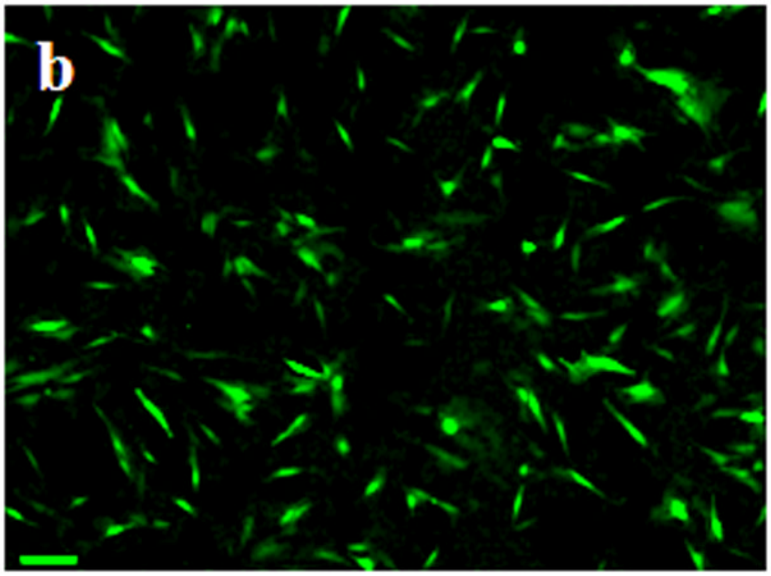
b

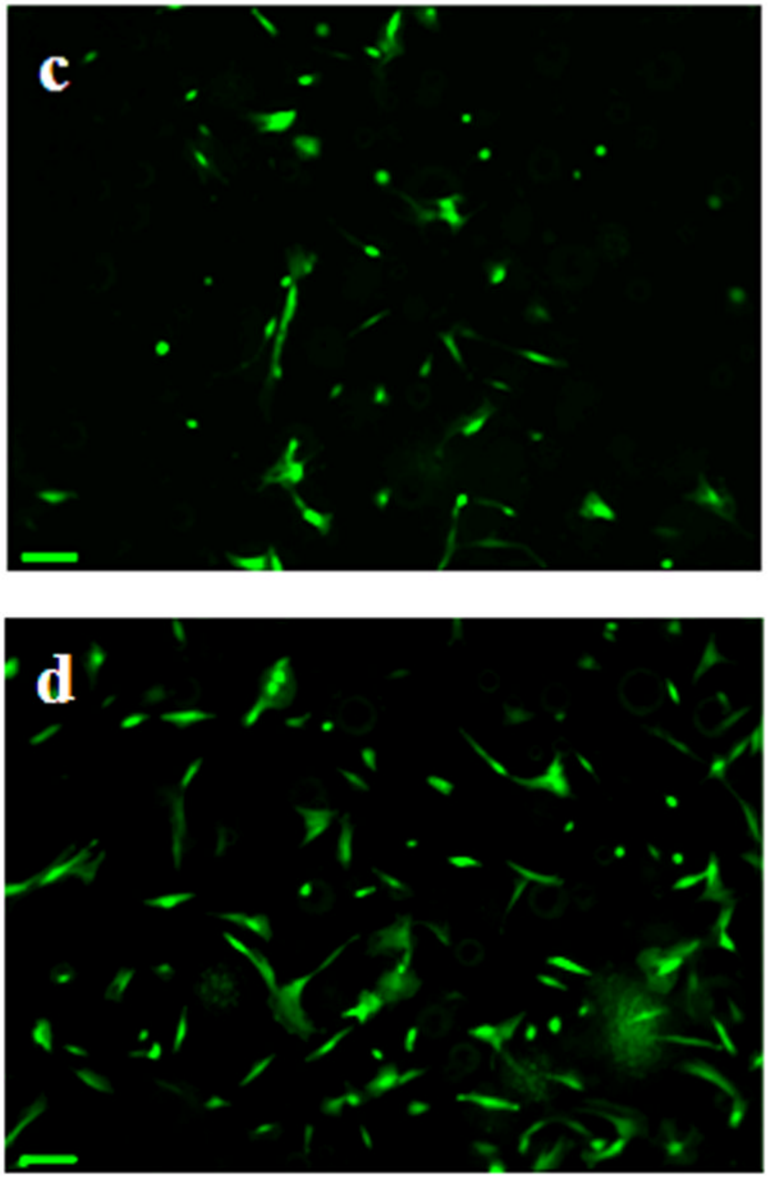
c
d

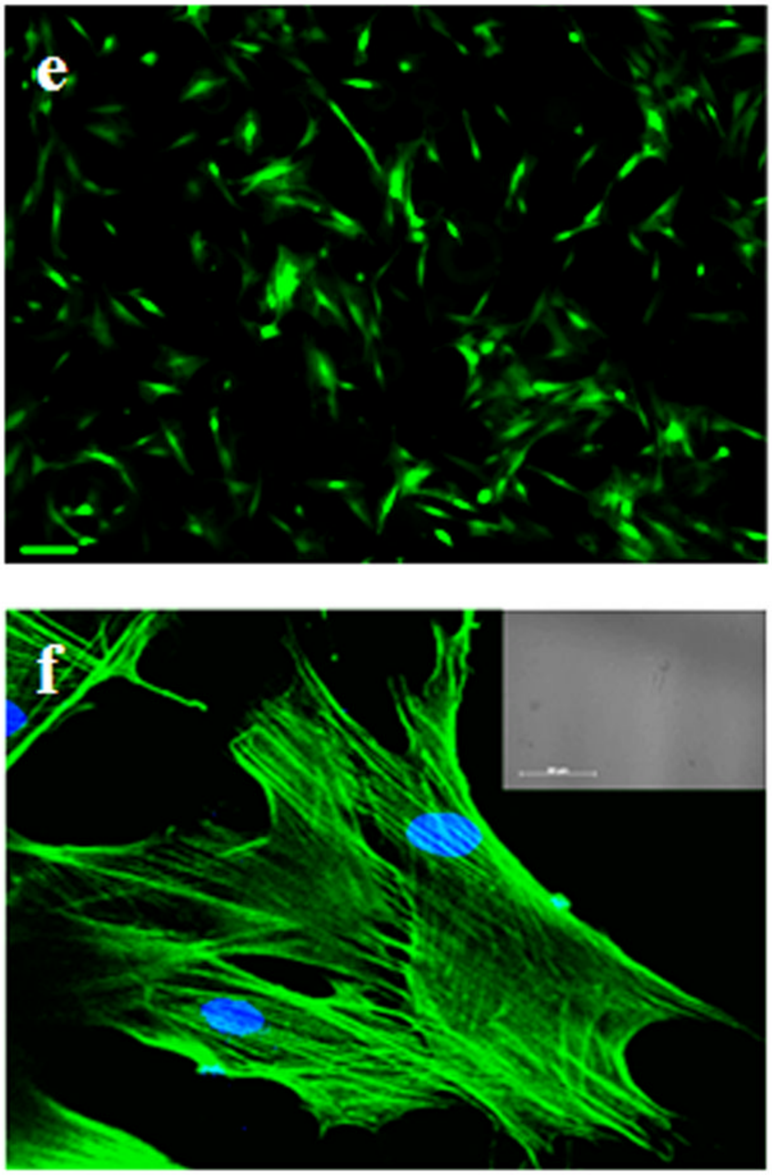
e
f

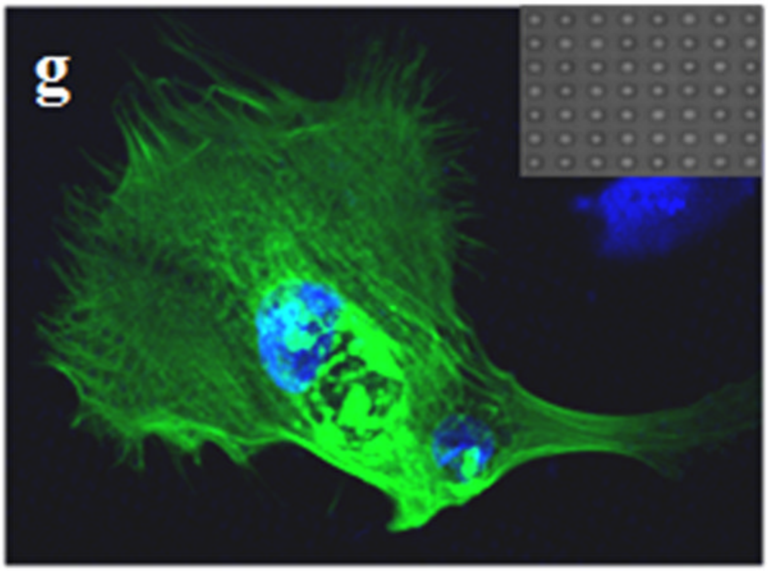

Figure 3.

a) Contact angle measurements for untreated (□) and oxygen plasma-modified (■) PCL planar surfaces. Fluorescent images of GFP-hMSCs cultured at 28 °C for 1 day on b)TCPS, c) untreated, d) oxygen plasma-treated, and e) oxygen plasma-Fn treated planar PCL surfaces. Immunofluorescent staining of hMSC actin (Green) cultured at 28 °C for 1 day on f) planar and on g) 2 μm cubic array PCL surfaces. DAPI nuclei counter-staining shown in blue. Scale bar is 100 μm.

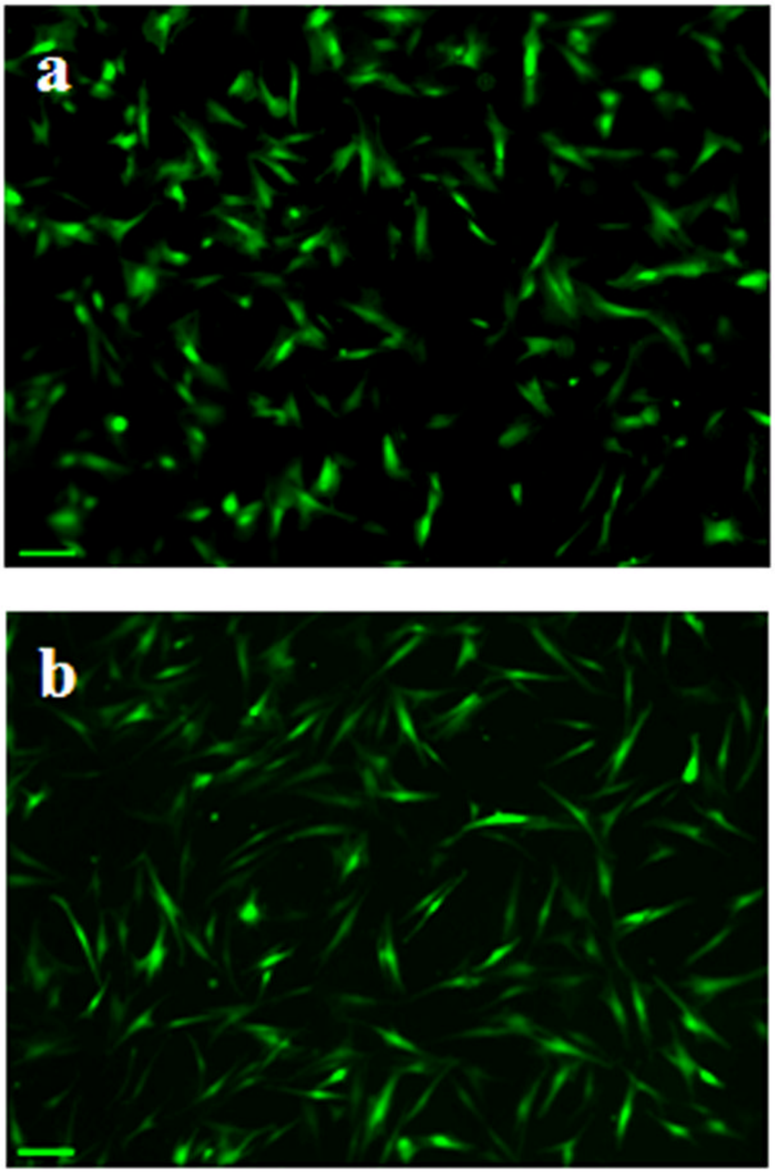
a
b

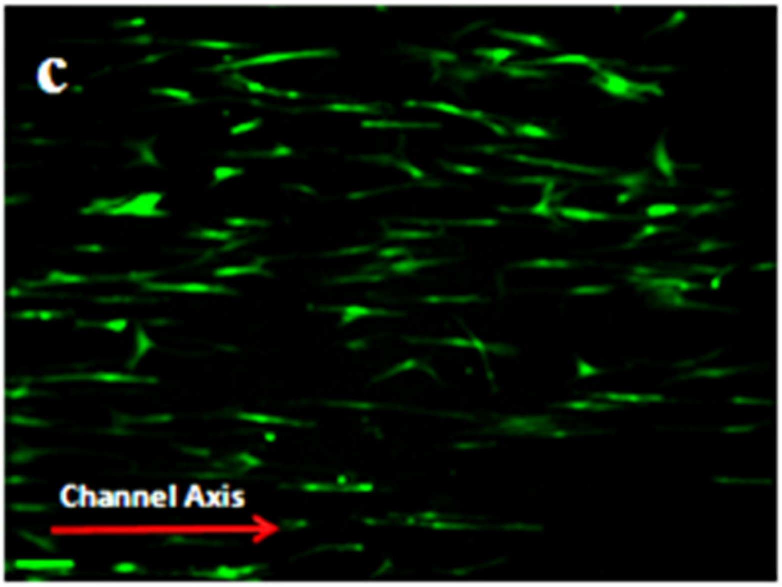
c
Channel Axis

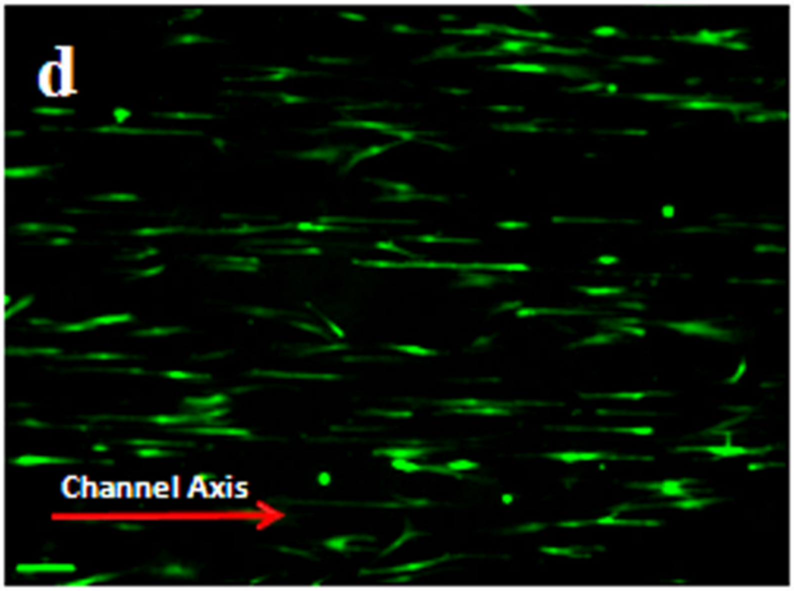
d
Channel Axis

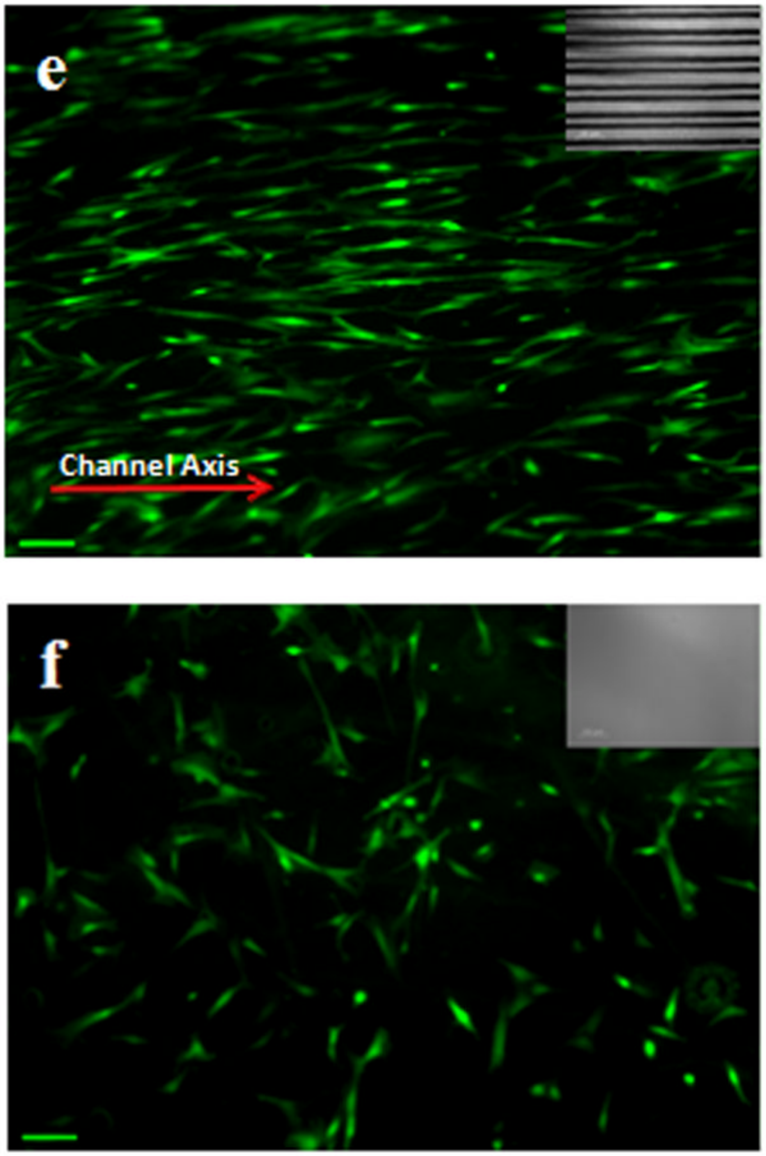

Figure 4.

GFP-hMSCs were cultured on static and dynamic PCL surfaces at 28 °C for 1 day and then subjected to 40 °C for 1 h. Subsequently, the cells were allowed to equilibrate for 12 h. Fluorescent images of GFP-hMSCs on static planar surfaces showed that the cells assumed a stellate shape (a) before and (b) after heat treatment. Images of cells cultured on static surfaces patterned with 3 × 5 μm channels showed that cell alignment was present (c) before and (d) after heat treatment. Cells cultured on (e) temporary 3 × 5 μm channel SMP arrays demonstrated significant alignment along the channel axis. However, when the substrate was heated and the surface shifted to (f) a flat topography, the cell morphology changed to stellate shaped in response to the surface transformation. Scale bar is 100 μm.

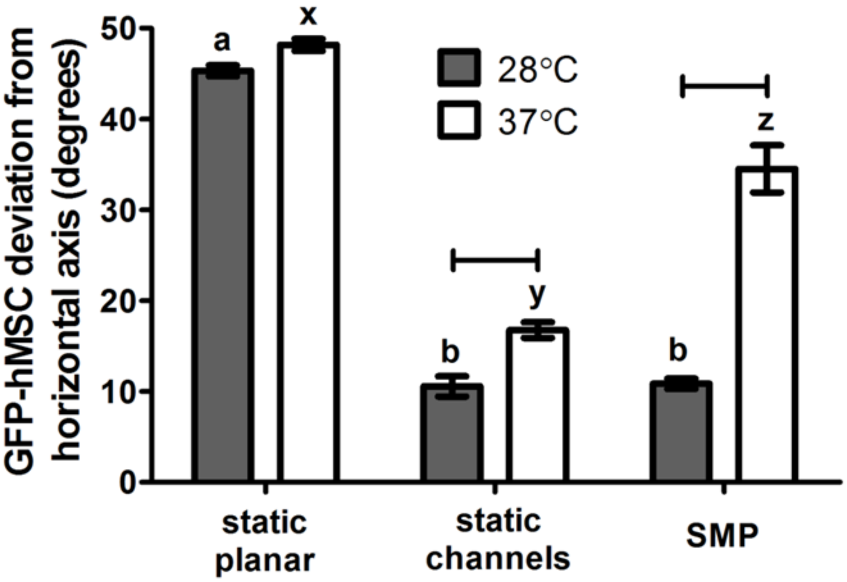

Figure 5.
Columns represent the average angle of deviation from the horizontal (channel) direction, with error bars depicting the standard error measurement for 3 images of 3 replicate substrates (n = 9). Letters a and b (x, y, and z) denote significant statistical differences between substrates at 28°C (37°C) by one-way ANOVA post-hoc testing ($p < 0.001$). Horizontal bars indicate significant differences of cell alignment on a given substrate between temperature conditions by Student's t-test ($p < 0.001$).